Quantification of Ultra-Widefield Retinal Images

True surface area and beyond.

BY DANIEL E. CROFT, BA; CHARLES C. WYKOFF, MD, PhD; DAVID M. BROWN, MD; JANO van HEMERT, PhD; AND MICHAEL VERHOEK, PhD

Advances in imaging periodically lead to dramatic changes in the diagnosis, management, and study of retinal disease. For example, the innovation and wide-spread application of fluorescein angiography and optical coherence tomography (OCT) have had tremendous impact on the management of retinal disorders.[1,2] Recently, ultra-widefield (UWF) imaging has opened a new window into the retina, allowing the capture of greater than 80% of the fundus with a single shot.[3] With montaging, much of the remaining retinal surface area can be captured.[4,5] However, to maximize the potential of these new modalities, accurate quantification of the pathology they capture is critical.

BACKGROUND

The Early Treatment Diabetic Retinopathy study defined one of the first standards by which investigators could quantify retinal pathology from fundus photography. The investigators divided the posterior pole into 7 standard fields, grids were overlaid on the macula to approximate area, and arbitrary scales were created to grade pathology (ie, capillary loss on a scale of 0 to 4).[6]

Today, UWF imaging is capable of capturing substantially greater fundus area than the 30° images of the posterior pole more typical of OCT modalities. Furthermore, digital imaging allows more precise, accurate, and automated data analysis. These advances necessitate a new methodology for retinal quantification. The primary challenge is correcting for the warping produced when the retina, a 3-dimensional (3-D), nearly spherical surface, is projected onto a 2-dimensional (2-D) plane for viewing and analysis. This effect is demonstrated by Mercator projections of the Earth, in which Greenland appears to be the size of South America, while it is actually only 12% of its size. By correcting for this warping inherent to UWF imaging, it is possible for fundus pathology to have an objective metric.

"The primary challenge is correcting for the warping produced when the retina, a 3-dimensional (3-D), nearly spherical surface, is projected onto a 2-dimensional (2-D) plane for viewing and analysis."

Yet surface area alone may not be sufficient to characterize many retinal pathologies. The enormous variability in the functional relevance and metabolic demand across the retina suggests that area measured in square millimeters may not be the only relevant unit. To optimally predict the biological activity of retinal disease, it may also be necessary to quantify histology in affected regions.

This article describes our approach to these issues.[5]

MONTAGING

A method was first developed to standardize montages derived from 5 component UWF images (optomaps) taken with the Optos 200Tx SLO at different directionally guided gaze angles (ie, the patient was guided to look off-axis in order to image all 4 quadrants of the retina). The gaze angle at which each component image was taken was then calculated based on the location of the fovea. Using

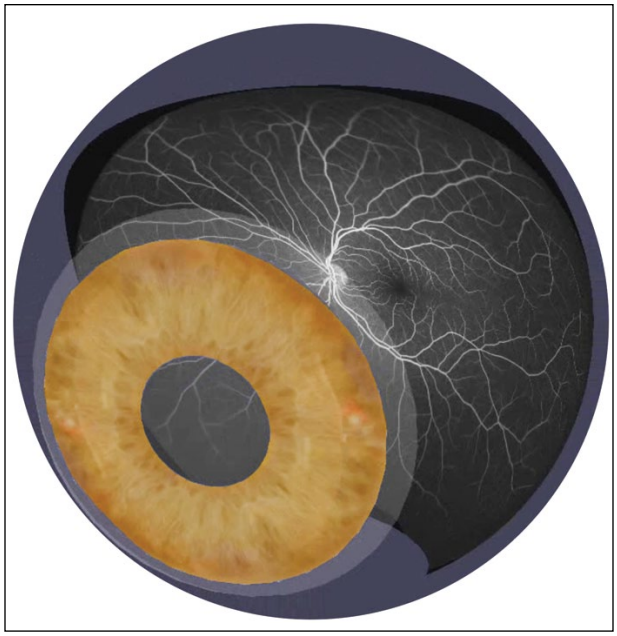

Figure 1. On-axis fluorescein angiogram optomap projected to its anatomically correct location on a 3-D model eye.

this information, each component image was individually projected to its anatomically correct location on a 3-D model eye of standard dimensions. This stereographic projection was performed by ray tracing every pixel through a combined optical model of the Optos 200Tx SLO and the Navarro UWF model eye.[7] This optical model represented the projection utilized by the Optos 200Tx SLO platform to create the initial 2-D optomap. By reversing this device-specific projection, an accurate anatomic representation of the image on the 3-D model eye was created (Figure 1).

For each component image, its 3-D representation was then mapped back to a 2-D stereographic projection, but this time onto a standard 4000 x 4000-pixel canvas. This stereographic projection was conformal and, hence, preserved shape.

This seemingly redundant conversion from 2-D to 3-D and then back to 2-D for each component image was necessary to create standardized projections on a registered canvas. Thus, each pixel on the canvas correlates with a specific anatomic location on the 3-D model eye. The fovea is always at the center.

To complete the montage, the 4 eye-steered images—superior, inferior, nasal, and temporal—were registered 1-by-1 to the on-axis image. Due to the UWF nature of the images, significant overlap occurred between quadrants. Image registration between a pair of images first extracted their vasculature and subsequently applied rotational affine translation with cross correlation (ie, an algorithm

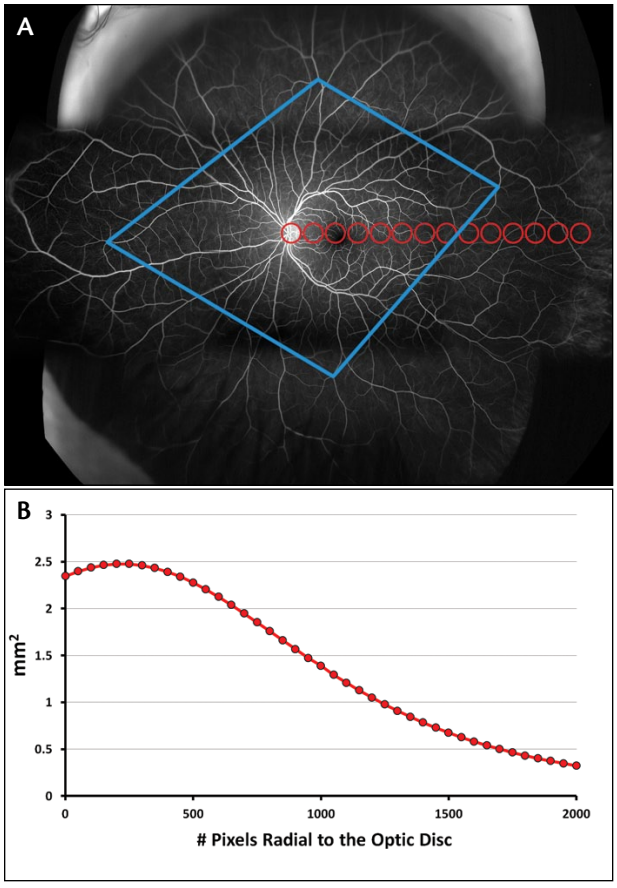

Figure 2. Precision of montaging was assessed by quantifying the area within the blue quadrilateral defined by 4 vascular landmarks across 10 unique montages (A). Distortion was assessed by quantifying the area represented by the red circles, translated from the optic disc, radially towards the periphery (A and B).

slightly rotated the peripheral images to align vasculature). Finally, segments were blended together to create a contiguous montage (Figure 2A).

QUANTIFICATION

Following standardization of the montages, a method to quantify retinal surface area in square millimeters was developed and automated. Each pixel in the registered canvas was individually projected to its anatomically correct location on the 3-D model eye, and spherical trigonometry was applied to calculate its respective surface area in square millimeters. This created a table for defining the surface area values for each pixel in the registered canvas based on its undistorted 3-D representation. Thus, when a user selects regions of a montage to quantify, the corresponding surface-area values of all the selected pixels are simply added together.

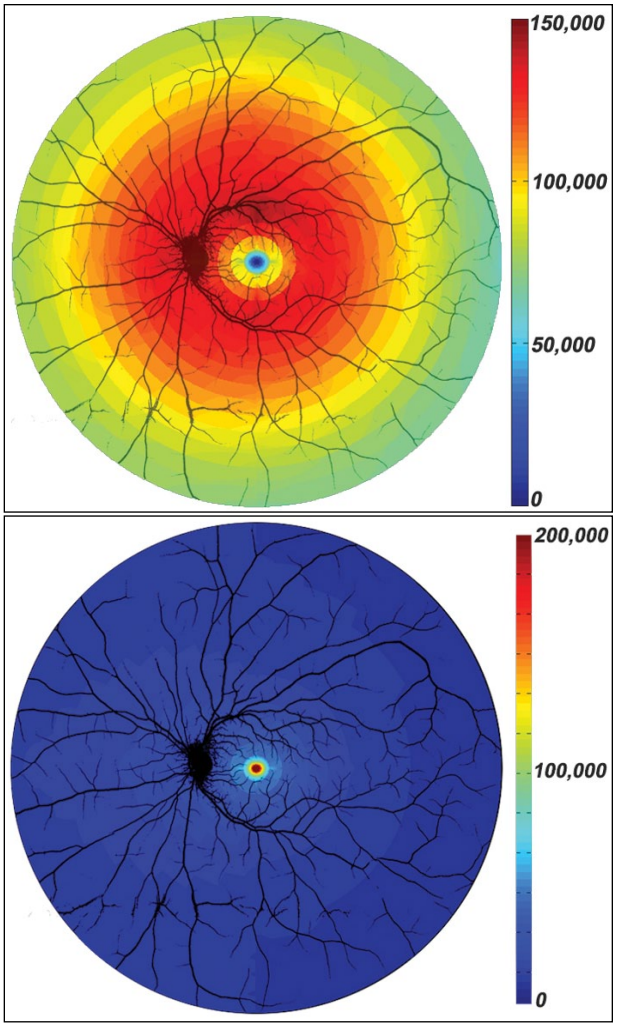

Figure 3. Cone photoreceptor density map interpolated from histology data (cones/mm^2) (top). Rod photoreceptor density map interpolated from histology data (rods/mm^2) (bottom).[8]

To assess the precision of montaging and quantification, 10 separate fluorescein angiograms (FA) were performed over a 2-month period on an anatomically stable, healthy eye. A montage was produced from each of these FA sessions, and 4 vascular landmarks were selected, 1 in each quadrant of the completed montage. A line was drawn between each of these 4 landmarks to create a standardized quadrilateral, and the area inside was subsequently quantified in each montage (Figure 2A, blue quadrilateral). The mean area of the quadrilateral quantified across the 10 unique FA montages was 408.97 mm^2 with a relative standard deviation of 0.7%, reflecting a high degree of precision in montaging and quantification.

To assess accuracy, the mean disc area of 50 patients was quantified and compared to a published standard of normative disc-area measurements.[9] The mean disc area

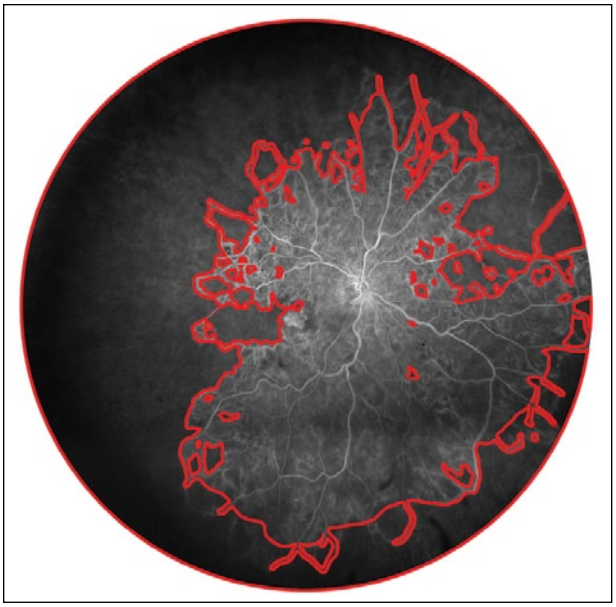

Figure 4. Quantifying peripheral capillary dropout in an eye with a severely ischemic central retinal vein occlusion. Red lines delineate regions selected for quantification.

quantified from 50 patients in the current work fell within the published accepted range at 2.21 mm^2. Effectively assessing accuracy was challenging, as there are no peripheral landmarks with accepted dimensions for comparison. True accuracy would require in vivo or postmortem measurements to correlate with fundus images. This is currently in development.

To illustrate why approaching the retina as a 3-D object is so crucial to quantification, the distortion inherent to these UWF images was plotted. The optic disc in a selected montage was determined to have a radius of 49 pixels. In its native location, this circle of pixels represented a disc area of 2.35 mm^2. This same circle of pixels was then translated radially toward the periphery and quantified every 50 pixels. After crossing the posterior pole, the circle represented less and less surface area the further away it was located. The circle represented only 0.50 mm^2 upon reaching the ora serrata (~1700 pixels away), a nearly 5-fold difference from its native location (Figure 2A, red circles; and Figure 2B).

NOT ALL RETINAS ARE CREATED EQUAL

In 1968, Esterman published a grid to score visual fields.[10] His novel system to grade peripheral vision based on relative functional importance, known as the Esterman grid, quickly replaced its predecessor, which only quantified area.[11] It was this insight that not all retinas are created equal that inspired us to further refine the retinal surface area quantification methodology described above: Because surface area alone is insufficient to characterize retinal

"Because surface area alone is insufficient to characterize retinal pathology from a functional or metabolic perspective, a method was developed to quantify affected histology."

pathology from a functional or metabolic perspective, a method was developed to quantify affected histology.

First, the densities of photoreceptor rods and cones from previously published histology data were mapped onto the 3-D model eye.[8] Then, density maps of the retina were generated by interpolating these sampled data points over the surface of the sphere via inverse distance weighted averaging in MATLAB 2013a, a computational modeling and analysis software (Figure 3). This effectively estimated the photoreceptor density at any given pixel by calculating the distance (arc length) to the 8 surrounding sampled histology points. A weighted average of the densities of these 8 surrounding points was then applied to reflect their respective distance to the pixel being interpolated. These density maps were then integrated with the area measurement methodology described above. Thus, after selecting a region of the retina from a montage, the area was calculated and then multiplied by the respective photoreceptor densities in that region to generate the approximate number of selected rods and cones.

To illustrate the potential clinical application of this, 3 different metrics were employed to grade nonperfusion in a patient with significant retinal ischemia secondary to central retinal vein occlusion (Figure 4). Out of a field size of 3 461 472 pixels, 2 111 694 pixels were identified as nonperfused. Uncorrected for warping, this simple pixel ratio represents 61% nonperfusion. Utilizing the quantification methodology described above, this grading field represents 691.9 mm^2 of retinal surface area, with 374.8 mm^2 of nonperfusion. Corrected for warping, this represents 54% nonperfusion. Quantified in relation to affected photoreceptors, the grading field covers approximately 77 025 041 photoreceptors (3 419 783 cones and 73 605 258 rods), with approximately 36 443 157 photoreceptors (1 550 571 cones and 35 892 586 rods) nonperfused. This histology ratio represents 47% nonperfusion.

CONCLUSION

This proof-of-concept analysis is only the beginning, as additional histology data will be integrated into this quantification tool. Ultimately, the goal is to create a weighted metabolic retinal index, which may more accurately predict the biological activity of retinal pathology. In the future, a relevant metabolic retinal index could be tailored to fit the context of the pathology being studied. ■

Daniel E. Croft, BA, is a research coordinator at Retina Consultants of Houston. He is enrolling at Baylor College of Medicine, Houston, Texas and will be pursuing an MD PhD in pharmacology. Mr. Croft specializes in computational analysis and may be reached at daniel.croft@houstonretina.com.

Charles C. Wykoff, MD, PhD, is co-director of the Greater Houston Retina Research Foundation, practices at Retina Consultants of Houston, and is a clinical assistant professor of ophthalmology at Weill Cornell Medical College, Houston Methodist Hospital, Texas. He is a member of the Retina Today *Editorial Board. Dr. Wykoff may be reached at ccwmd@houstonretina.com.*

David M. Brown, MD, is director of the Greater Houston Retina Research Foundation and practices at Retina Consultants of Houston and the Houston Methodist Hospital in Houston, Texas. He is a member of the Retina Today *Editorial Board. Dr. Brown may be reached at dmbmd@houstonretina.com.*

Jano van Hemert, PhD, is the imaging research manager and academic liaison at Optos Plc. He holds an MSc in computer science and a PhD in mathematics and physical sciences. Dr. van Hemert may be reached at jvanhemert@optos.com.

Michael Verhoek, PhD, is a computer scientist at Optos Plc. He holds an MSc in theoretical physics, an MSc degree in information processing and neural networks, and a PhD in medical image analysis. Dr. Verhoek may be reached at mverhoek@optos.com.

1. Novotny HR, Alvis DL. A method of photographing fluorescence in circulating blood in the human retina. *Circulation*. 24:82-86.
2. Huang D, Swanson EA, Lin CP, et al. Optical coherence tomography. *Science*. 1991;254(5035):1178-1181.
3. Manivannan A, Plskova J, Farrow A, et al. Ultra-wide-field fluorescein angiography of the ocular fundus. *Am J Ophthalmol*. 2005;140:525-527.
4. Spaide RF. Peripheral areas of nonperfusion in treated central retinal vein occlusion as imaged by wide-field fluorescein angiography. *Retina*. 2001;31:829-837.
5. Croft DE, van Hemert J, Wykoff CC, et al. Precise montaging and metric quantification of retinal surface area from ultra-widefield fundus photography and fluorescein angiography. *Ophthalmic Surg Lasers Imaging Retina*. In Press.
6. Early Treatment Diabetic Retinopathy Study Research Group. Classification of diabetic retinopathy from fluorescein angiograms. *Ophthalmology*. 1991;98:807-822.
7. Escudero-Sanz I, Navarro R. Off-axis aberrations of a wide-angle schematic eye model. *J Opt Soc Am A Opt Image Sci Vis*. 1999;16(8):1881-1891.
8. Curcio CA, Sloan KR, Kalina RE, Hendrickson AE. Human photoreceptor topography. *J Comp Neurol*. 1990. 292:497-523.
9. Samarawickrama C, Hong T, Jonas JB, et al. Measurement of normal optic nerve head parameters. *Surv Ophthalmol*. 2012;57(4):317-336.
10. Esterman B. Grid for scoring visual fields. *Arch Ophthalmol*. 1968;79:400-406.
11. Committee on Rating of Mental and Physical Impairment. Guide to the evaluation of permanent impairment; the visual system. *JAMA*. 1958;168:475-485.